

Field-induced ferroelectric and commensurate spin state in multiferroic HoMn_2O_5

H. Kimura,^{1,*} Y. Kamada,¹ Y. Noda,¹ K. Kaneko,² N. Metoki,² and K. Kohn³

¹*Institute of Multidisciplinary Research for Advanced Materials, Tohoku University, Sendai 980-8577, Japan*

²*Advanced Science Research Center, Japan Atomic Energy Agency, Tokai, Ibaraki 319-1195, Japan*

³*Department of Physics, Waseda University, Tokyo 169-8555, Japan*

(Dated: September 13, 2018)

Neutron diffraction measurements under high magnetic fields have been performed for the multiferroic compound HoMn_2O_5 . At zero field, high-temperature incommensurate magnetic (HT-ICM) – commensurate magnetic (CM) – low-temperature incommensurate magnetic (LT-ICM) orders occur with decreasing temperature, where ferroelectric polarization arises only in the CM phase. Upon applying a magnetic field, the LT-ICM phase completely disappears and the CM phase is induced at the lowest temperature. This field-induced CM state is completely associated with the field-induced electric polarization in this material [Higashiyama *et al.*, Phys. Rev. B **72**, 064421 (2005).], strongly indicating that the commensurate spin state is essential to the ferroelectricity in the multiferroic RMn_2O_5 system.

PACS numbers: 61.12.Ld, 64.70.Rh, 75.47.Lx, 75.80.+q

Cross-correlations among different extensive (or intensive) variables have been one of the most important issues from both scientific and technological points of view. Among them, the correlation between magnetic and dielectric properties, which is actualized as a magnetoelectric (ME) effect, has recently drawn much attention and been studied intensively. Although the ME effect, where an electric polarization induced by a magnetic field or inversely a magnetization induced by an electric field, has been predicted since a long time ago[1], the magnitude of the ME effect has been too small to reply to an industrial demand thus far. However, it has recently been found that RMnO_3 and RMn_2O_5 (R = rare earth, Bi, or Y) systems show a colossal ME effect[2, 3], which provides new candidate materials for multifunctional devices such as a magnetically controlled ferroelectric memory. Numerous studies have revealed that these materials show a “multiferroic” behavior, where magnetic and dielectric orders coexist in almost the same temperature range and their order parameters strongly couple with each other[4, 5, 6]. However, the microscopic properties of the antiferromagnetism and ferroelectricity as well as their relevance to the colossal ME effect have not been fully understood yet. To clarify them, we have studied the magnetic and dielectric properties of the RMn_2O_5 system using a neutron diffraction technique. Our systematic studies for RMn_2O_5 compounds with R = Er, Y, Tb and Tm have revealed that the incommensurate–commensurate phase transition for Mn^{3+} and Mn^{4+} spin structures strongly correlates with a ferroelectric phase transition[6, 7, 8, 9, 10, 11, 12].

Recently, Higashiyama *et al.* reported the effects of magnetic field on the dielectric properties of the HoMn_2O_5 compound[13]. They found that the magnetic field along the b -axis induced a spontaneous electric polarization, indicating that the ferroelectricity in the RMn_2O_5 system is magnetically driven. However, to

clarify the origin of field-induced ferroelectricity, a microscopic investigation for magnetic properties as well as for the lattice distortion that arises from the ferroelectricity is indispensable. In this work, we thus performed a neutron diffraction study under a magnetic field for a HoMn_2O_5 single crystal to establish the magnetic phase diagram for the spin structure and its relevance to the dielectric phase diagram. Our measurements reveal that the incommensurate–commensurate phase transition on the spin structure occurs when the magnetic field is applied along the b -axis, showing that the commensurate spin state is essential to the ferroelectricity in HoMn_2O_5 .

A single crystal of HoMn_2O_5 was grown by a PbO – PbF_2 flux method[14]. The size of the crystal was about 100 mm^3 . Neutron diffraction measurements were performed using the thermal neutron triple-axis spectrometer TAS-2 installed at JRR-3M in the Japan Atomic Energy Agency. The sample was mounted on the $(h \ 0 \ l)$ scattering plane with a vertical-field superconducting magnet, which results in applying a field along the b -axis perfectly. The incident and final energies of neutrons were fixed at 14.3 meV using a pyrolytic graphite (PG) (002) monochromator and an analyzer. A PG filter was inserted in front of the sample to reduce higher-order contamination. The experimental configuration was 15° – 80° – 80° – 80° . In the field cooling process, we applied the magnetic field at 60 K, far above T_N . We also performed magnetic structure analysis at the commensurate magnetic phase under zero magnetic field using an identical HoMn_2O_5 single crystal. Details of the structure analysis involving the results for Ym_2O_5 and ErMn_2O_5 will be published elsewhere[15].

HoMn_2O_5 has an orthorhombic structure with $Pbam$ symmetry at room temperature, where edge-sharing Mn^{4+}O_6 octahedra align along the c -axis and pairs of Mn^{3+}O_5 pyramids link the Mn^{4+}O_6 chains in the ab -plane[16]. The $4f$ -moment of Ho^{3+} , and the $3d$ -moment

of Mn^{4+} and Mn^{3+} ions are responsible for the characteristic magnetism in this system. In zero magnetic field, we have obtained magnetic and dielectric properties analogous to those of other RMn_2O_5 compounds reported previously[7, 8, 9, 10, 11, 12]. Figure 1(a) shows dielectric constant as a function of temperature, where two phase transitions are seen apparently at ~ 39 K ($\equiv T_{C1}$) and ~ 20 K ($\equiv T_{C2}$). It was reported that the spontaneous polarization along the b -axis grows up below T_{C1} , whereas the polarization becomes weaker or almost vanishes below T_{C2} [13]. In this paper, we respectively call the intermediate T phase between T_{C1} and T_{C2} , and the lowest T phase below T_{C2} , the FE and X phases, as defined in Ref. [13]. The temperature dependence of the intensity of magnetic Bragg peaks is shown in Fig. 1(b). Filled and open symbols indicate the intensity observed at incommensurate and commensurate \mathbf{Q} positions, respectively. As seen in Fig. 1(b), a high-temperature incommensurate magnetic (HT-ICM) phase appears (closed triangles) below T_N and disappears at T_{C1} , where the commensurate magnetic (CM) phase (open circles) and the ferroelectric (FE) phase arises concurrently. On further cooling, the CM phase vanishes and a low-temperature incommensurate magnetic (LT-ICM) phase (closed circles) emerges around T_{C2} , where the spontaneous polarization becomes almost zero[13]. The inset in Fig. 1(b) shows the \mathbf{Q} position of the magnetic Bragg peak denoted with a propagation wave vector $\mathbf{q} = (q_x \ 0 \ q_z)$ in three different magnetic phases. Note that the minor CM phase persists even below T_{C2} , which coexists with the major LT-ICM phase. Both the dielectric and magnetic phase diagrams as functions of temperature are schematically shown in the middle panel of Fig. 1.

On applying the magnetic field along the b -axis up to 13 T, the spin structure at the lowest temperature markedly changes. Figure 2 shows contour maps of LT-ICM and CM Bragg intensities around $\mathbf{Q} = (\frac{1}{2} \ 0 \ 2-\frac{1}{4})$ at $T = 4$ K, taken under zero field and $H = 13$ T. These maps correspond to slices along the $(h \ 0 \ l)$ reciprocal plane. At zero field, as seen in Fig. 2(a), two peaks are found at the incommensurate position described as the propagation vector of $\mathbf{q} \sim (\frac{1}{2} \pm 0.019 \ 0 \ \frac{1}{4} + 0.022)$. However, when the magnetic field of 13 T is applied on the field cooling (FC) process, the two incommensurate peaks completely disappear and a single peak appears exactly at the commensurate position, shown in Fig. 2(b). Figure 2(c) shows the data taken at 13 T with the zero-field cooling (ZFC) process, where the incommensurate peaks still persist. The difference between the peak distribution in the FC process and that in the ZFC process means that there is a large hysteresis at the incommensurate–commensurate phase transition, suggesting the first-order nature of the phase transition. The first-order nature is also seen in the dielectric phase transition between the FE and X phases[13]. This one-to-

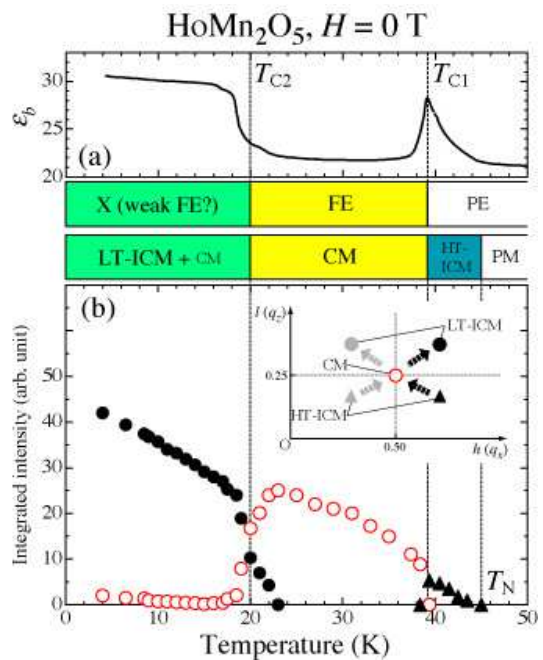


FIG. 1: (Color online) Temperature dependences of (a) dielectric constant along b -axis and (b) integrated intensities of LT-ICM (filled circles), CM (open circles), and HT-ICM (filled triangles) Bragg peaks, taken at $H = 0$ T. The middle part of this figure shows a schematic phase diagram for dielectric and magnetic properties. Positions of magnetic peaks (propagation wave vectors q_x, q_z) in LT-ICM, CM, and HT-ICM phases are depicted in the inset of Fig. 1(b).

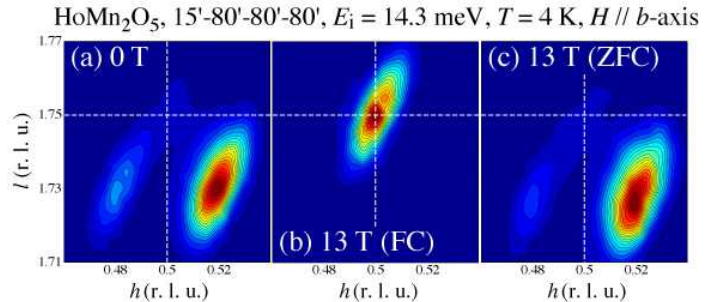


FIG. 2: (Color online) Intensity maps of LT-ICM and CM Bragg peaks around $(\frac{1}{2} \ 0 \ 2-\frac{1}{4})$ in $(h \ 0 \ l)$ zone at $T = 4$ K. Data was taken under (a) $H = 0$ T, (b) $H = 13$ T in field cooling (FC), and (c) $H = 13$ T in zero-field cooling (ZFC). The magnetic field was applied along the b -axis.

one correspondence between the magnetic and dielectric properties clearly shows that the FE phase is magnetically induced.

The detailed field dependences of order parameters for the LT-ICM, HT-ICM, and CM phases are summarized in Fig. 3. All the data were taken in the FC process up to $H = 13$ T. Figure 3(a) shows the temperature dependence of intensity for LT- and HT-ICM Bragg peaks. The behavior of the HT-ICM signal at around 40 K, in-

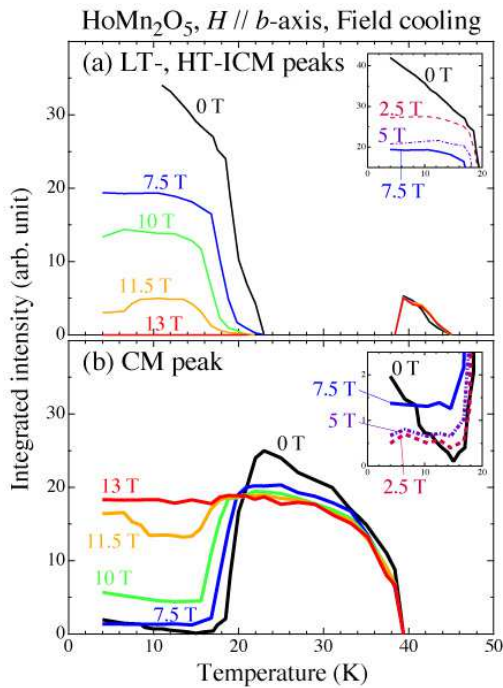


FIG. 3: (Color online) Temperature dependence of integrated intensity for (a) LT-ICM, HT-ICM and (b) CM Bragg peaks, taken under $H = 0$ T and $7.5 \leq H \leq 13$ T. Insets show enlarged views of the data below $T = 20$ K and $0 \leq H \leq 7.5$ T.

volving the appearance and disappearance temperatures and the intensity variation, is completely independent of magnetic field. In contrast, the appearance temperature of the LT-ICM peak and its intensity decrease with increasing field. As for the CM signal shown in Fig. 3(b), the appearance temperature (T_{C1}) and the evolution of the order parameter above ~ 20 K do not change significantly, whereas the intensity of the signal below ~ 20 K is enhanced with increasing magnetic field. The field dependence for LT-ICM and CM signals becomes marked in the region between 10 T and 13 T, where both phases coexist and the fraction of intensity in each phase changes with field. This behavior indicates that incommensurate-commensurate magnetic phase transition has a strong first-order nature, which is consistent with the large hysteretic behavior seen in Fig. 2. The insets of Fig. 3 show the detailed temperature dependence below $T = 20$ K under magnetic fields between 0 T and 7.5 T. At zero field, not only the major LT-ICM but also the minor CM phases evolve with decreasing temperature. However, above $H = 2.5$ T, the temperature evolutions of both phases are almost saturated. Although the details are not clarified yet, this behavior might indicate the field response related with a Ho^{3+} moment induced by the ordering of Mn^{3+} and Mn^{4+} moments. Indeed, the magnetic structure analysis under zero field using the identical single crystal shows that Ho^{3+} moments of up

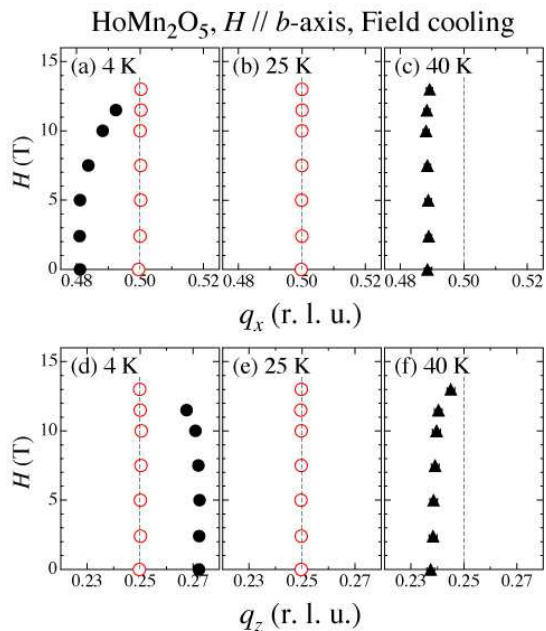


FIG. 4: (Color online) Field dependence of propagation wave vector $\mathbf{q} = (q_x \ 0 \ q_z)$ taken at $T = 4$ K, 25 K, and 40 K. (a)-(c), and (d)-(f) correspond to the results for q_x and q_z components, respectively. Filled circles, open circles, and filled triangles denote the data from LT-ICM, CM, and HT-ICM peaks, respectively.

to $\sim 1.3\mu_B$ are induced even at 25 K (CM phase)[15].

A magnetic propagation wave vector described by $\mathbf{q} = (q_x \ 0 \ q_z)$ as a function of magnetic field and temperature was measured. Figure 4 shows the field dependence of \mathbf{q} taken at $T = 4$ K, 25 K, and 40 K, corresponding to the LT-ICM, CM, and HT-ICM phases under zero field, respectively. The results for q_x and q_z components appear on the upper panels (Figs. 4(a)–(c)) and the lower panels (Figs. 4(d)–(f)), respectively. It is clearly seen that as magnetic field increases, the \mathbf{q} vectors for the CM and HT-ICM phases (open circles and filled triangles) are almost field independent, whereas those for the LT-ICM phase (filled circles) approach a commensurate position, indicating that the LT-ICM phase becomes unstable due to the development of the CM phase. It should be noted that the q_z component at 40 K also comes close to the $1/4$ position at $H = 13$ T. This might indicate that a one-dimensionally modulated ICM order is induced by the magnetic field, the phase of which was observed in ErMn_2O_5 [8] and YMn_2O_5 [9] at zero field.

To overview the correlation between the field response of the microscopic magnetic property and that of the dielectric property, we mapped out the magnetic field (H) – temperature (T) phase diagram for LT-ICM, CM, and HT-ICM states. Figure 5 shows the contour map of the intensities of the magnetic signals as functions of temperature and magnetic field only in the FC process. Boundaries between each phase are roughly indicated by white

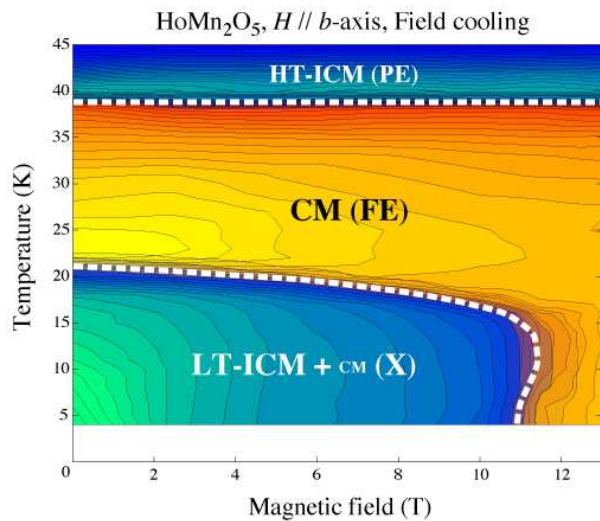


FIG. 5: (Color online) $H-T$ phase diagram for ICM and CM states in HoMn_2O_5 , shown as the contour map of intensity for ICM and CM magnetic signals. The dielectric phase diagram taken by Higashiyama *et al.*(ref. [13]) is superposed in this figure.

dashed lines. Distributions for each phase are expressed by a gradation sequence. The obtained phase diagram apparently shows that HT-ICM is completely field independent, whereas the LT-ICM phase rapidly disappears and the CM phase is induced around $H \sim 11$ T. Comparing our $H-T$ phase diagram with the dielectric phase diagram[13], it is quite interesting that the LT-ICM and CM phases in the magnetic property perfectly correspond to the null or weak ferroelectric (X) phase and the robust ferroelectric (FE) phase, respectively. These experimental facts evidently establish that the commensurate spin state is indispensable to the ferroelectricity, and thus the dielectric property in this system has a magnetic origin.

Our results have shown that the magnetic field strongly affects the magnetism below ~ 20 K (T_{C2} at zero field), whereas the magnetism above ~ 20 K is almost field independent. This strongly suggests that the $4f$ -moment of rare-earth atoms, of which amplitude becomes larger as temperature decreases, significantly contributes to the field responses in the magnetic and dielectric properties. Actually, as many studies have reported, a large ME effect has been found only in the lower-temperature region (LT-ICM phase at zero field)[13, 17]. Recent symmetric analysis of the magnetic structure for (Tb,Ho,Dy) Mn_2O_5 has shown that the magnetic interaction in Mn^{3+} and Mn^{4+} sublattices is geometrically frustrated[18, 19]. Such magnetic frustration might induce a competing magnetic ground state, that can be easily tuned by the $f-d$ spin exchange interaction between R^{3+} and $\text{Mn}^{3+,4+}$ ions. Our magnetic structure analysis in the CM phase of (Y,Er,Ho) Mn_2O_5 single crystals also clarified that the magnetic structure of Mn ions is com-

mon regardless of the existence of the f moment[6, 15]. Combining these results with the present observation of the field-induced CM state in HoMn_2O_5 , it is strongly suggested that the commensurate magnetic ground state in Mn ions is indispensable to the ferroelectricity in $R\text{Mn}_2\text{O}_5$ compounds.

Microscopic mechanisms of the magnetically driven ferroelectricity have been theoretically proposed with various frameworks such as exchange striction[20] and Dzyaloshinskii-Moriya (D-M) interaction[21, 22]. However, all the predictions do not require the commensurate spin state. The detailed magnetic and crystal structure analyses in both LT-ICM and CM phases are essential for completing the microscopic correlation between the magnetic and dielectric properties of the multiferroic $R\text{Mn}_2\text{O}_5$ system.

In summary, we have found the magnetic-field-induced commensurate spin state in HoMn_2O_5 . The field evolution of the commensurate ground state completely traces the development of the ferroelectric phase. Incommensurate-commensurate phase transition has a first-order nature, which is also consistent with a first-order ferroelectric phase transition. This study has microscopically shown that the commensurate spin state is essential to the ferroelectricity in the $R\text{Mn}_2\text{O}_5$ system.

We thank M. Matsuda and Y. Shimojo for technical assistance in operating the superconducting magnet. This work was supported by a Grant-In-Aid for Scientific Research (B), No. 16340096, from the Japanese Ministry of Education, Culture, Sports, Science and Technology.

* kimura@tagen.tohoku.ac.jp

- [1] P. Curie, J. Phys. (Paris), Colloq. **3**, 393 (1894).
- [2] T. Kimura, *et al.*, Nature (London) **426**, 55 (2003).
- [3] N. Hur, *et al.*, Nature (London) **429**, 392 (2004).
- [4] T. Goto, *et al.*, Phys. Rev. Lett. **92**, 257201 (2004).
- [5] I. Kagomiya, *et al.*, Ferroelectrics **280**, 131 (2002).
- [6] Y. Noda, *et al.*, J. Kore. Phys. Soc. **42**, S1192 (2003); Y. Noda, *et al.*, Physica B (2006) in press.
- [7] I. Kagomiya, *et al.*, J. Phys. Soc. Jpn. **70**, S145 (2001).
- [8] S. Kobayashi, *et al.*, J. Phys. Soc. Jpn. **73**, 1031 (2004).
- [9] S. Kobayashi, *et al.*, *ibid.*, 1593 (2004).
- [10] S. Kobayashi, *et al.*, *ibid.*, 3439 (2004).
- [11] S. Kobayashi, *et al.*, J. Phys. Soc. Jpn. **74**, 468 (2005).
- [12] S. Kobayashi, *et al.*, J. Kore. Phys. Soc. **46**, 289 (2005).
- [13] D. Higashiyama, *et al.*, Phys. Rev. B **72**, 064421 (2005).
- [14] B. Wanklyn, J. Mater. Sci., **7**, 813 (1972).
- [15] H. Kimura *et al.*, unpublished.
- [16] S. C. Abrahams and J. L. Bernstein, J. Chem. Phys. **46**, 3776 (1967).
- [17] N. Hur, *et al.*, Phys. Rev. Lett. **93**, 107207 (2004).
- [18] L. C. Chapon, *et al.*, Phys. Rev. Lett. **93**, 177402 (2004).
- [19] G. R. Blake, *et al.*, Phys. Rev. B **71**, 214402 (2005).
- [20] J. B. Goodenough, Phys. Rev. **100**, 564 (1955); J. Kanamori, J. Phys. Chem. Solids **10**, 87 (1959).
- [21] H. Katsura, *et al.*, Phys. Rev. Lett. **95**, 057205 (2005).

[22] I. A. Sergienko and E. Dagotto, cond-mat/0508075.